

# Volumetric Imaging Using 2D Capacitive Micromachined Ultrasonic Transducer Arrays (CMUTs): Initial Results

Ömer Oralkan<sup>1,2</sup>, A. Sanli Ergun<sup>1</sup>, Ching-Hsiang Cheng<sup>1</sup>, Jeremy A. Johnson<sup>1,3</sup>,  
Mustafa Karaman<sup>4</sup>, Thomas H. Lee<sup>2</sup>, and Butrus T. Khuri-Yakub<sup>1</sup>

<sup>1</sup>Edward L. Ginzton Laboratory, <sup>2</sup>Center for Integrated Systems, <sup>3</sup>Image Guidance Laboratory  
Stanford University, Stanford, CA 94305, U.S.A.

<sup>4</sup>Department of Electrical Engineering, Işık University, Istanbul, Turkey

*Abstract* – This paper presents the first volumetric images obtained using a 2D CMUT array with through-wafer via interconnects. An 8×16-element portion of a 32×64-element array flip-chip bonded onto a glass fanout chip was used in the experiments. This study experimentally demonstrates that 2D CMUT arrays can be fabricated with high yield using silicon micromachining processes, individual electrical connections can be provided using through-wafer interconnects, and the flip-chip bonding technique can be used to integrate the dense 2D arrays with electronic circuits for practical imaging applications.

## I. INTRODUCTION

3D ultrasound has been an extensive area of research for both medical and underwater imaging applications. Conventionally, 3D ultrasound images have been reconstructed from multiple 2D image planes obtained by mechanically scanning a 1D linear transducer array in the elevation direction. This method is too slow to allow real-time imaging of dynamic structures such as a beating heart. Another disadvantage of this approach is the poor spatial resolution in the elevation direction. The electronic scanning of a volume using a 2D array greatly speeds up the data acquisition and provides uniform resolution in both azimuthal and elevational directions. However, there are some major difficulties which has limited the feasibility of 3D ultrasound imaging using 2D arrays. A 2D array consists of a large number of small transducer elements to achieve a good resolution without violating the spatial sampling criterion in both azimuthal and elevational directions. The acoustic power output and receiving sensitivity of 2D array elements are limited because of the small size of the elements. There are also severe difficulties in fabricating these densely populated 2D arrays and providing individual electrical connections to each element.

CMUT technology is a strong candidate to overcome the technical challenges outlined above [1]. CMUTs are fabricated using standard silicon integrated circuit (IC) fabrication technology, and therefore it is possible to fabricate large arrays using simple photolithography. Individual electrical connections to transducer elements in these arrays are provided by through-wafer interconnects. 2D

CMUT arrays having as many as 128×128 elements have already been successfully fabricated and characterized [2]. Besides the ease of manufacturing CMUTs, there are major performance advantages such as improved bandwidth and sensitivity, and potential for electronic integration. We have previously reported the fabrication process for 1D and 2D CMUT arrays. We have also characterized these arrays in terms of the performance of a single element in transmit and receive modes [3], [4]. We have recently demonstrated the first full scale phased array images using a 128-element linear array based on CMUT technology [5].

In this paper, we present the first volumetric images obtained using a 2D CMUT array with through-wafer via interconnects. An 8×16-element portion of a 32×64-element array has been used along with a 128-channel data acquisition system. Section II briefly describes the 2D CMUT arrays used in this study. The experimental methods used are explained in Section III. The results are presented in Section IV.

## II. 2D CMUT ARRAYS

The basic building block of CMUTs is a capacitor cell which consists of a metalized membrane suspended over a heavily doped silicon substrate (Fig. 1). In the case of 2D CMUT arrays, the bottom electrode for each transducer element is an island of doped polysilicon so that bottom electrodes of different elements would be isolated from each other. The fabrication process for 2D CMUT arrays with through-wafer via interconnects is described in detail in [2]. The physical dimensions of the 2D CMUT array used in this work are listed in Table I.

## III. EXPERIMENTAL WORK

We diced a 128×128 2D CMUT array fabricated on a 4-inch wafer into smaller arrays with 32×64 elements in order to flip-chip bond it onto a glass carrier chip (Fig. 2(a)). The current goal for integration is to flip-chip the transducer array onto a silicon die with integrated transmit/receive circuits. In this experiment, we used a glass fanout chip that provides individual leads from the elements to the pads surrounding the array. The

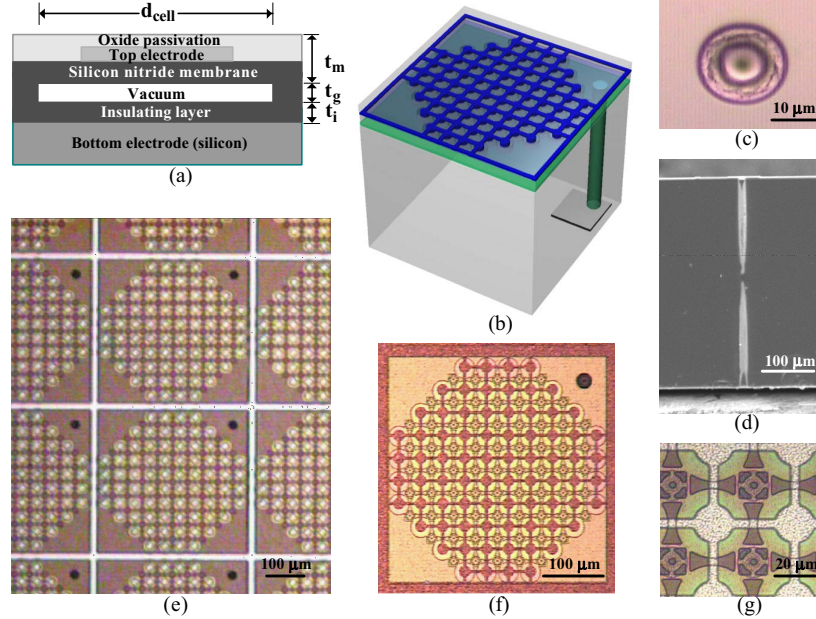


**Figure 1.** 2D CMUT array. (a) Schematic cross-section of a CMUT cell. (b) 3D visualization of a CMUT cell with a through wafer via interconnect. (c) Top view of a through wafer via. (d) SEM cross-section of a through wafer via. (e) Top view of a portion of a 2D CMUT array. (f) Top view of a single 2D CMUT array element. (g) Top view of individual CMUT cells constituting 2D array elements.

32×64-element CMUT array was bonded onto the fanout chip. This particular fanout chip that we used in this experiment enables access to a 16×16-element portion of the 32×64-element array. The CMUT array-glass substrate assembly is mounted and wire-bonded onto a PCB. The bonded 2D CMUT array is shown in Fig. 2.

The PC-based data acquisition system used in this study included custom designed circuits and a software interface. The experimental setup shown in Fig. 3 was originally designed and used in 2D imaging experiments with 1D CMUT arrays. This data acquisition system is capable of handling 128 channels. Therefore, an 8×16 part of the 2D array was used in the experiments described here. Due to the use of board-level electronics, the parasitic capacitance is more than 20 pF, whereas the device capacitance is only 1 pF. To improve the SNR of the collected A-scans, we transmitted from a synthesized powerful virtual element by connecting 4×4 elements (at the center of the 8×16 array) in parallel without any phasing. The remaining elements in the array were used for receive. The received signals were amplified with a 60-dB gain amplifier, and digitized at a rate of 100 MHz, with 8-bit sample

resolution. 100 successive acquisitions were averaged to form each echo signal. The received echo spectrum from the spherical phantom was centered at 5 MHz with a fractional bandwidth of 100%. The DC bias voltage on the 2D CMUT array was set to 20 V and a 15-V, 100-ns rectangular pulse was used to excite the 4×4-element, un-phased transmit subarray at the center of the 8×16 2D array.

Two different imaging phantoms were submerged in vegetable oil: a 2.37-mm steel sphere located 10 mm from the array; and two 12-mm thick Plexiglas plates located 20-mm and 60-mm from the array.

#### IV. RESULTS

The 3D images were reconstructed using the synthetic phased array approach. However, due to the use of a fixed transmit aperture with no phasing, receive-only dynamic beamforming was employed. After the individual voxel values were calculated, a 40-dB logarithmic compression was employed on the volume data and the volumetric image was visualized by surface rendering. Fig. 4 shows the reconstructed 3D image of the parallel-plate phantom. The four interfaces from two Plexiglas plates are clearly identified in the images. The cross-section images in elevation and azimuth directions are displayed with a dynamic range of 40 dB in Fig. 4(a) and (c), respectively.

The images obtained from the spherical phantom are shown in Fig. 5. The experimental and simulated results are in good agreement for main-, side-, and grating-lobes. The grating lobes indicate the violation of the spatial sampling criterion in this case where the element pitch is 420 μm, and the frequency of operation is 5 MHz.

TABLE I  
PHYSICAL PARAMETERS OF THE 2D CMUT ARRAY

Element pitch ( $d$ ), μm	420
Size of an element, μm	400×400
Number of cells in the element	76
Cell diameter ( $d_{cell}$ ), μm	36
Membrane thickness ( $t_m$ ), μm	0.65
Gap thickness ( $t_g$ ), μm	0.1
Insulating layer thickness ( $t_i$ ), μm	0.2
Substrate thickness, μm	500

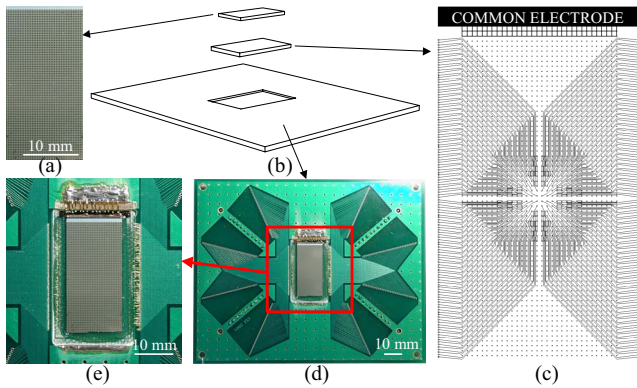


**Figure 2.** 2D array assembly. (a) 32 x 64 2D CMUT array. (b) Schematic representation of 3D multichip assembly. (c) Top view of the carrier chip layout to fan out a 16x16 portion of the 2D CMUT array. (d) The PCB carrying the flip-chip-bonded 2D array-glass substrate assembly. (e) Magnified view of the center portion of the PCB showing the wire bonds from glass substrate to the PCB.

## V. CONCLUSION

In this paper, we presented the first volumetric imaging results using 2D CMUT arrays. In spite of the use of a suboptimal experimental setup and a small portion of the 2D CMUT array, the results obtained are encouraging. This study experimentally demonstrated that 2D CMUT arrays can be fabricated with high yield using silicon micromachining processes, individual electrical connections can be provided using through-wafer interconnects, and the flip-chip bonding technique can be used to integrate these dense 2D arrays with electronic circuits for practical imaging applications.

## ACKNOWLEDGEMENTS

This work was supported by the United States Office of Naval Research. Flip-chip bonding was performed by the Lockheed-Martin Corporation through the DARPA Sonoelectronics research program.

## REFERENCES

- [1] B. T. Khuri-Yakub, C.-H. Cheng, F. L. Degertekin, S. Ergun, S. Hansen, X. C. Jin, and Ö. Oralkan, "Silicon micromachined ultrasonic transducers," *Jpn. J. Appl. Phys.*, vol. 39, pp. 2883-2887, May 2000.
- [2] C. H. Cheng, A. S. Ergun, and B. T. Khuri-Yakub, "Electrical through wafer interconnects with 0.05 picofarads parasitic capacitance on 400- $\mu\text{m}$  thick silicon substrate," in *Proc. Solid-State Sensor, Actuator and Microsystems Workshop*, 2002, pp. 157-160.
- [3] X. C. Jin, Ö. Oralkan, F. L. Degertekin and B. T. Khuri-Yakub, "Characterization of one-dimensional capacitive micromachined ultrasonic immersion transducer arrays," *IEEE Trans. on Ultrason. Ferroelect. Freq. Contr.*, vol. 48, pp. 750-759, May 2001.
- [4] Ö. Oralkan, X. C. Jin, F. L. Degertekin and B. T. Khuri-Yakub, "Simulation and experimental characterization of a 2-D capacitive micromachined ultrasonic transducer array element," *IEEE Trans. Ultrason. Ferroelect. Freq. Contr.*, vol. 46, pp. 1337-1340, Nov. 1999.
- [5] O. Oralkan, A. S. Ergun, J. A. Johnson, M. Karaman, U. Demirci, K. Kaviani, T. H. Lee, and B. T. Khuri-Yakub, "Capacitive micromachined ultrasonic transducers: Next generation arrays for acoustic imaging?," *IEEE Trans. Ultrason. Ferroelect. Freq. Contr.*, in press.

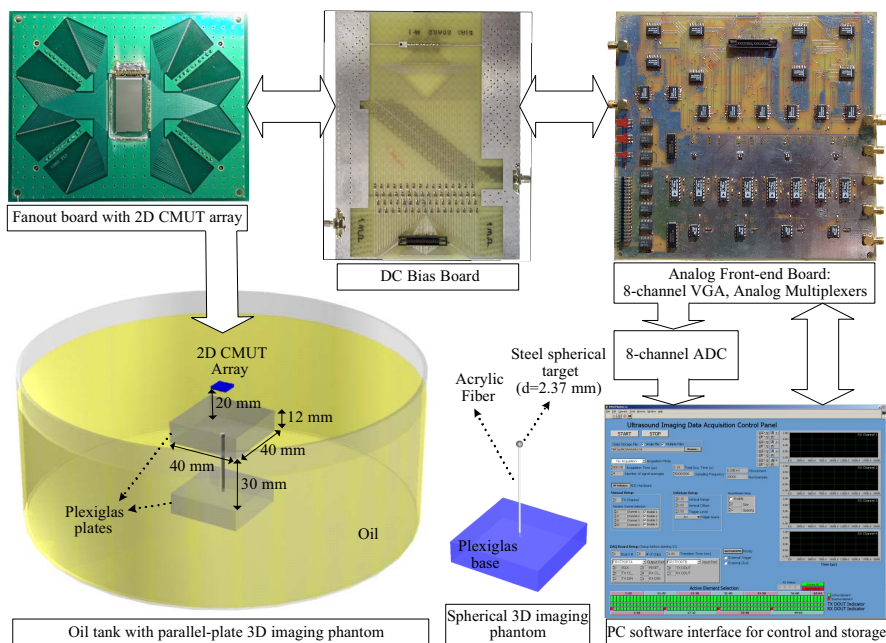


**Figure 3.** Experimental setup with 3D imaging phantoms.

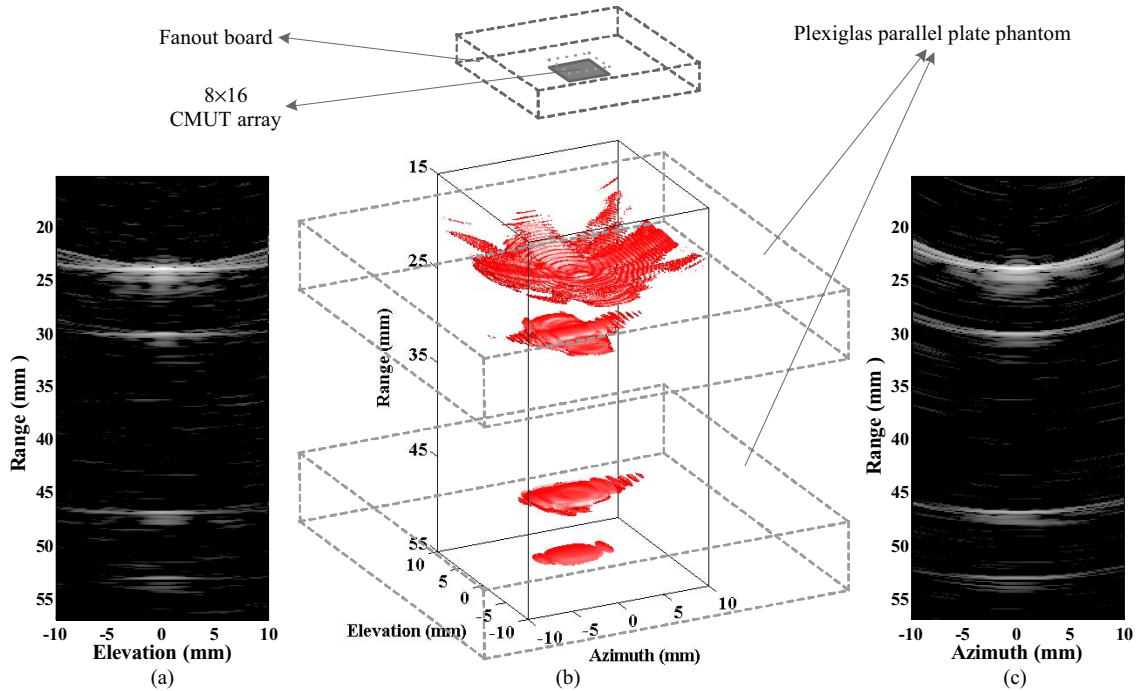


**Figure 4.** Reconstructed 3D image of the parallel plates phantom. (a) Elevational grayscale cross-section image with a display dynamic range of 40 dB. (b) Surface-rendered 3D image superimposed on the parallel plate phantom figure. (c) Azimuthal grayscale cross-section image with a display dynamic range of 40 dB.

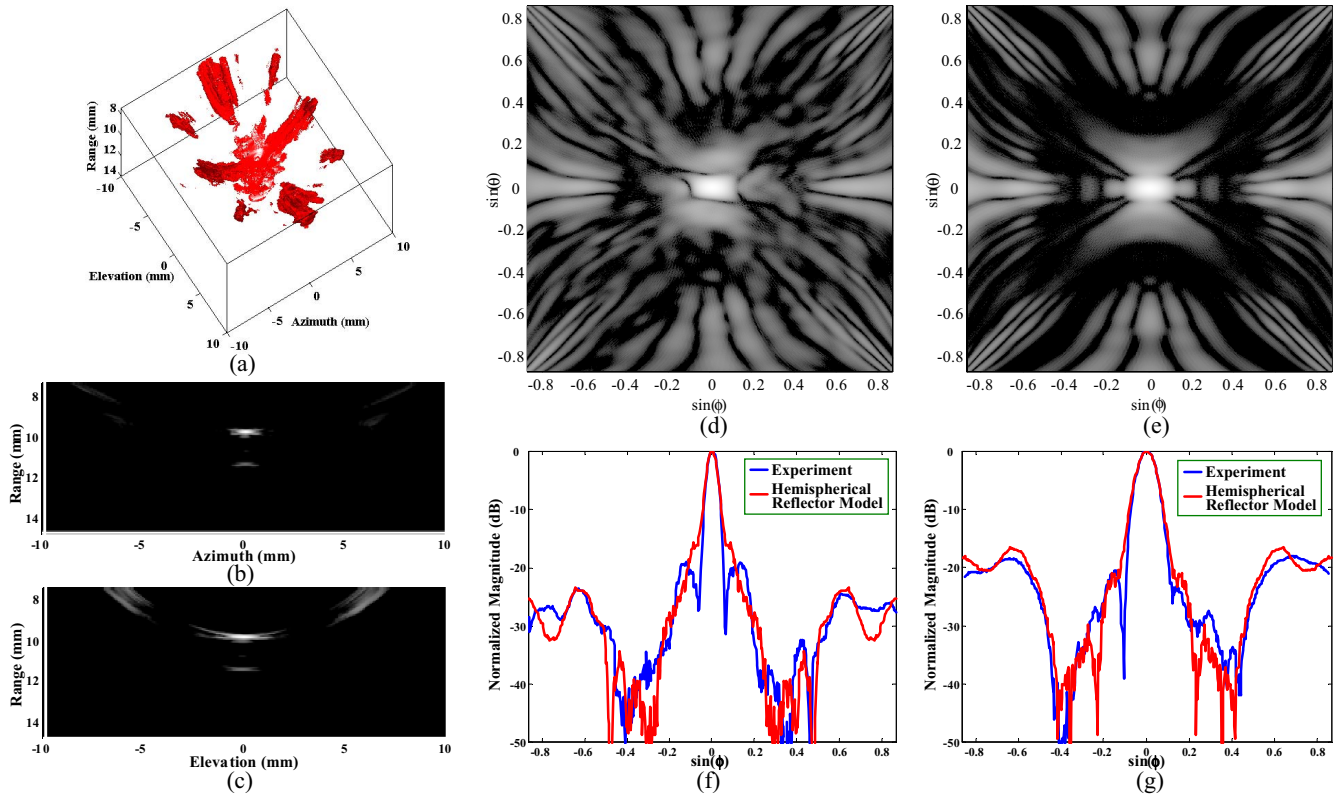


**Figure 5.** Images of the spherical phantom. (a) Surface-rendered visualization of the spherical phantom. (b) Side-view from elevation direction (DR= 20 dB). (c) Side-view from azimuth direction (DR= 20 dB). (d) Constant-range cross-section image (Experimental, DR=40 dB). (e) Constant-range cross-section image (simulation with hemispherical reflector model, DR=40 dB). (f) Azimuthal cross-section of the constant-range images. (g) Elevational cross-section of the constant-range images.